Journal Home Page: https://sjes.univsul.edu.iq/

Research Article:

Hydraulic performance of Submerged Flow over Rectangular Labyrinth Weirs with Round Corners

Ahang S. Ali [1,a,*]
Kawa Z. Abdulrahman [2,a]
Wazira E. Qadir [3,a]
[a] **University of Sulaimani , College of engineering , Water Resources Dept. , Sulaimani , KR, Iraq**

Article Information

Article History:
Received: December 22nd , 2025
Accepted : March, 31st , 2026
Available online: April , 2026

Keywords:
Rectangular labyrinth weir, hydraulic performance, discharge coefficient, submergence level

About the Authors:
Corresponding author:
Ahang Salah Ali
E-mail: ahang.ali@univsul.edu.iq
Researcher Involved:
Prof. Dr. Kawa Z. Abdulrahman
E-mail: kawa.abed@univsul.edu.iq
Wazira Ezzat Qadir
E-mail: wazera.qadir@univsul.edu.iq

DOI https://doi.org/10.17656/sjes.10206

Abstract

This experimental study investigates the hydraulic performance of rectangular labyrinth weirs with rounded corners under both free-flow and submerged-flow conditions. Nine rectangular labyrinth weirs, varying in height and crest length, were constructed from High-Density Polyethylene Plastic (HDPE) and tested in a laboratory flume under a range of discharges (0.0028-0.034 m^3/s). The effects of geometry and tailwater depth on discharge efficiency were evaluated. The results indicated that the discharge coefficient (C_L) generally increases with the relative head ratio (H_T/P) up to a certain point (0.12-0.26), after this point, the discharge coefficient declines. Additionally, the discharge efficiency of rectangular labyrinth weirs with rounded corners decreases as the degree of submergence increases. Models with greater weir height were less sensitive to submergence, while those with longer crest lengths exhibited greater efficiency losses. Overall, labyrinth weirs with rounded corners maintain favorable performance under a wide range of discharges. These findings provide new insight into the influence of crest geometry and submergence on labyrinth weir hydraulics.

1. Introduction

A labyrinth weir is a type of linear weir designed with a folded shape in plain view to increase the crest length within the same channel or spillway width. Labyrinth weir allows weir to handle higher flow rates at lower water head levels compared to conventional linear weirs of similar width. Due to their efficient hydraulic properties and flexible design, labyrinth weirs are commonly used in streams, canals, rivers, ponds, and reservoirs for purposes such as regulating headwater levels, dissipating energy, aerating flow, and serving as spillways [1]. Weir structures are generally designed to operate under free-flow conditions, where the tailwater surface remains below the crest of the weir. In such conditions, the relationship between the discharge and the weir head is mainly influenced by the weir's geometry and the characteristics of the approaching flow. However, when the tailwater level rises above the crest, the weir becomes submerged. Under submerged conditions, a higher upstream head is required to maintain the same discharge as in free-flow conditions. Submergence is more likely to occur when low-head control structures are placed in rivers or canals with mild slopes, especially if there are downstream obstructions or dense vegetation [2,3]. The hydraulic performance of labyrinth weirs with submerged flow has been previously assessed. The first serious investigations into the labyrinth weirs were conducted by Taylor

(1968) [5]. Taylor (1968) [5] evaluated the performance of labyrinth weirs by comparing their discharge ratios with those of linear weirs, providing design curves that relate the effective head on the weir to the flow depth. Generally, Taylor (1968) observed that the magnification factor for submergence flow was greater than that for free-flow conditions. According to literature, submergence effects have a smaller impact on labyrinth weirs compared to linear weirs [2,4,5]. This paper explores the hydraulic behavior of labyrinth weirs under free flow and submerged flow conditions. It focuses on discharge efficiency and how submergence affects the head-discharge relationship. By analyzing these factors, the study provides insights into how labyrinth weirs behave compared to traditional structures.

2. Materials and Methods

To conduct this study, nine rectangular labyrinth weirs were designed and installed in a laboratory flume (S6MKII – Teaching and Research Flume, produced by the Armfield company) at the University of Sulaimani. The weir models, with walls 1 cm thick, were constructed using High-Density Polyethylene Plastic (HDPE). The rectangular labyrinth weir models featured rounded corners and flat crest shapes. Three different weir heights (150 mm, 200 mm, and 250 mm) and three distinct effective lengths (160 mm, 310 mm, and 460 mm) were tested. For all experimental runs (8 runs), the slope of the steel bed in the flume (measuring 5 m in length, 0.3 m in width, and 0.45 m in depth, with Plexiglas sidewalls) was maintained at zero. Figures (1 and 2) provide sketches of the models and the flume, while Table (1) details the specifications of the models analyzed in this study. The models, placed in the middle of the flume in inverse orientation, were then tested under different steady-state conditions without artificial aeration devices. The steady discharges, ranging from 0.003 to 0.03 m3/s, were measured by an ultrasonic flowmeter. For each discharge, a point gauge, 0.1 mm accuracy, was used to measure the depth of water flowing over the crest of the models, h, as illustrated in Figure (3). Each experimental run, lasting 3 to 4 hours, visual observations and digital-photo taking (figure 4) were used to document the hydraulic performance of the models. Initially, tests were conducted under free-flow conditions, followed by submerged flow conditions, which were achieved using three rectangular weirs with varying heights (5 cm, 10 cm, and 15 cm) but the same width (30 cm). The details of the experiments are presented in Tables (2-5).

3. Result and Discussion:

In this experimental study, the hydraulic performance of nine rounded-corner one-cycle rectangular labyrinth weirs were evaluated under both free-flow and submerged-flow conditions. To determine the coefficient of discharge for the weirs, the head-discharge correlations shown below were used [5,7].

$$Q = \frac{2}{3} * \sqrt{2g} * C_L * L_C * H_T^{1.5} \quad (1)$$

$$Q = \frac{2}{3} * \sqrt{2g} * C_B * B * \left(h + {V_a^2}/{2g}\right)^{1.5} \quad (2)$$

Where Q is the discharge of the flow over the labyrinth weir, g is the gravitational acceleration, C_L and C_B are the coefficients of discharge (dimensionless coefficients), L_C is the centerline length of the weir crest (effective length), B is the width of the channel (flume), H_T is the total head on the crest of the models, H_s is the height of sill (see Figure 3), h is the depth of water flowing over the weir crest, and V_a is the approach (average cross-sectional) velocity for the flow upstream of the weir. To assess the influence of submergence, the models were subjected to varying tailwater depths, H_s (50 mm, 100 mm, and 150 mm above the channel bed), and their performance was compared with free-flow conditions. Figure 4. shows the photographs of all models tested for the same water depth, h = 70 mm. Figures 5–13 and Tables 3 to 5 illustrate the variations of discharge coefficient, C_L, with respect to H_T/P for each individual model, while Figure (5) summarize the effect of weir submergence depth.

3.1 Hydraulic Performance of the Models

From the results, the discharge efficiency of rectangular labyrinth weirs decreases as the degree of submergence increases, which means that submerged flow conditions require a higher upstream head to maintain the same discharge compared to free-flow conditions. From Figures (5 to 13), for all models tested, the discharge coefficient initially increased with HT/P by nearly ≈ 0.12 – 0.26, after which it began to decrease. This trend is consistent with the findings of previous studies [1, 6, 7]. Under submerged conditions, however, the decrease in CL was more pronounced, reflecting the reduction in effective head resulting from the increasing tailwater [8]. Figures (5–13) clearly show that higher submergence levels (HS = 100 mm and 150 mm) produced reductions in CL compared to the free-flow

or lower submerged case (HS = 50 mm).From Figure 5, for model M1, CL increased with HT/P up to 0.16 in the free flow condition, then gradually decreased as HT/P rose further. At 5 cm submergence level, the curve followed a similar trend but with slightly lower values (9% on average), while at 10 cm submergence level, discharge efficiency dropped by about 21% on average as a reference with free flow condition. At 15 cm submergence level, the values of *C*L go up until a certain point (HT/P = 0.2) after which *C*L remained nearly constant and very low (*C*L around 0.1– 0.11).

For model M2, Figure (6) shows the free flow condition exhibits the highest efficiency, with C_L rising steeply to about 0.3 near $H_T/P \approx 0.12$ before gradually declining at higher head ratios. At 5 cm submergence level, the curve shows a comparable trend while at 10 cm submergence level, the curve matches the free-flow values up to $H_T/P \approx 0.35$; after this point the line more decreases than the free flow condition by about %6 on average. The poorest performance occurs at 15 cm submergence, where C_L peaks near 0.3 but then drops rapidly and remains significantly lower than the other conditions. On average, C_L at 15 cm submergence lower than C_L at free flow condition by about 20%. In Figure (7), unlike the previous models, M1 and M2, the differences between free flow and submerged cases are less pronounced for model M3. Under free flow condition, the CL reaches a peak of about 0.29 around $HT/P \approx 0.12$ before gradually declining. The curves for 5 cm and 10 cm submergence levels closely overlap with the free flow case. Even at 15 cm submergence level, the coefficient remains relatively close to free flow, peaking near 0.29 and then following a similar downward trend. Overall, the results indicate that the M3 model is less sensitive to submergence depth compared to M1 and M2, as its discharge coefficient remains comparatively high and stable across all tested conditions. This is because M3 has a greater height (25 cm compared to 15 cm for M1), which provides a larger effective head and reduces the impact of tailwater. This is consistent with findings by Crookston (2012) [4], which showed that higher labyrinth weirs are less face to nappe interference and submergence effects. Models M4, M5, and M6, as well as models M7, M8, and M9, show a similar pattern, which was seen for models M1, M2, and M3, as illustrated in Figures (8 – 13) and Table (3). In all cases, the discharge coefficient CL increases with HT/P up to a certain value; after that, it decreases as HT/P increases. The only noticeable difference is that the value of CL decreases under both free and submerged cases when the crest length L_C increases (M4, M5, M6, M7, M8, and M9). At higher submergence levels (Hs = 10 cm and Hs = 15 cm), this reduction becomes more evident. The results show that longer labyrinth weirs are more sensitive to submergence effects, see Figures (8-13).

3.2 Effect of Submergence Levels

Submergence tests were conducted for each labyrinth weir models for various flow rates and submergence levels (H_s = 5, 10, and 15 cm). Figure (14) illustrates the variation of the discharge coefficient (C_L) with the relative total head (H_T/P) for different submergence stages at model 4 (M4), where the submergence head (HS) is taken as 5, 10, and 15 cm at a constant weir height of P = 15 cm. The results show that for models with H_S = 5 and 10 cm, C_L initially increases with H_T/P up to a certain point and then decreases with further increase in H_T/P. The maximum values of C_L (0.27) are observed at H_T/P = 0.2 ratio for model with H_S = 5 cm, after which the coefficient gradually declines. Among the tested submergence conditions, the highest C_L values are recorded for H_s = 5 cm, followed by H_s = 10 cm (C_L = 0.25), while the lowest C_L values are obtained for H_s = 15 cm. This behavior can be explained by the effect of submergence on weir hydraulics. The reduction in discharge efficiency under submerged conditions can be attributed to the increased energy dissipation caused by the interaction between the upstream and downstream flows. As the tailwater level rises above the weir crest, the downstream water level interferes with nappe aeration and reduces the effective head, thereby decreasing flow efficiency and lowering C_L. The findings of this study align with the findings of Taylor (1968), who observed that labyrinth weirs exhibit a smaller reduction in discharge efficiency under submerged conditions compared to linear weirs. However, the results differ slightly from those of Crookston and Tullis (2013), who reported higher discharge coefficients for trapezoidal labyrinth weirs under similar conditions. This discrepancy may be due to differences in weir geometry, particularly the rounded corners in the present study, which could have altered the flow dynamics. Additionally, the study by Tullis et al. (2007) emphasized the importance of weir height and crest length in determining discharge efficiency, which is consistent with the observations made in this study. The rounded corners of the weirs played a critical role in reducing localized turbulence and flow separation, which are common issues in sharp-cornered weirs. This design feature likely contributed to the relatively stable performance of the weirs under submerged conditions.

4. Conclusions

The hydraulic performance of nine rectangular labyrinth weirs with rounded corners was evaluated under both free-flow and submerged flow conditions. Laboratory flume tests were conducted with discharges between 0.00102 and 0.03357 m^3/s and water depths over the weir crest from 0.002 to 0.009 m. The total head over the weir (H_T/P) varied from 0.08 to 0.60, representing a broad range of flow conditions. For all models, the discharge coefficient increased with H_T/P from approximately 0.12 to 0.26, then decreased as H_T/P continued to rise. The laboratory experiments demonstrated that submergence has a significant effect on weir performance. Discharge efficiency decreased as the degree of submergence increased. The discharge coefficients (C_L) declined by up to 20-30 percent compared to free-flow conditions. The most substantial reductions occurred at higher tailwater levels (H_S = 150 mm submergence), where discharge coefficients dropped by up to 30 percent relative to free-flow conditions. These results indicate that rounded-corner labyrinth weirs perform effectively under both free-flow and submerged conditions. However, careful consideration of tailwater conditions is crucial during the design process. This study corroborates previous research on labyrinth weir hydraulics and provides new evidence that corner geometry is critical in reducing efficiency losses.

Reference

[1] Crookston BM, Tullis BP. Hydraulic design and analysis of labyrinth weirs. I: Discharge relationships. Journal of Irrigation and Drainage Engineering. 2013, 1;139(5):363-70.

[2] Tullis BP, Young JC, Chandler MA. Head-discharge relationships for submerged labyrinth weirs. Journal of hydraulic engineering. 2007,133(3):248-54.

[3] Vaughn T, Crookston BM. Influence of submerged woody debris at labyrinth weirs in river applications. River Research and Applications. 2022, 38(2):235-44.

[4] Crookston BM, Tullis BP. Labyrinth weirs: Nappe interference and local submergence. Journal of Irrigation and Drainage Engineering. 2012, 1;138(8):757-65.

[5] Taylor G. *The performance of labyrinth weirs* (Doctoral dissertation, University of Nottingham).1968.

[6] Roushangar K, Alami MT, Shiri J, Asl MM. Determining discharge coefficient of labyrinth and arced labyrinth weirs using support vector machine. Hydrology research. 2018, 1;49(3):924-38.

[7] Yousif OS, Abdulrahman KZ, Qadir W, Ali AS, Karakouzian M. Characteristics of flow over rectangular labyrinth weirs with round corners. Hydrology. 2021, 18;8(4):158.

[8] Azimi AH, Hakim SS. Hydraulics of flow over rectangular labyrinth weirs. Irrigation Science. 2019, 1;37(2):183-93.

الأداء الهيدروليكي للغمر الجريان فوق الهدارات المتعرجة المستطيلة ذات الزوايا المستديرة

المستخلص

تتناول هذه الدراسة التجريبية الأداء الهيدروليكي للهدارات المتشابكة المستطيلة ذات الزوايا المستديرة تحت ظروف الجريان الحر والجريان المغمور. تم تصنيع تسعة نماذج من الهدارات المتشابكة المستطيلة، تختلف في الارتفاع وطول الحافة، باستخدام البلاستيك عالي الكثافة(HDPE) ، وتم اختبارها في قناة مختبرية تحت مجموعة من التصاريف المختلفة .تم تقييم تأثير الشكل الهندسي وعمق الماء في المجرى السفلي على كفاءة التصريف. أظهرت النتائج أن معامل التصريف (CL) يزداد عادةً مع نسبة الرأس النسبي (HT/P) حتى نقطة معينة (من ٠.١٢ إلى ٠.٢٦) ، ثم يبدأ بالانخفاض بعدها بالإضافة إلى ذلك، تنخفض كفاءة التصريف للهدارات المتشابكة المستطيلة ذات الزوايا المستديرة مع زيادة درجة الغمر .كما تبين أن النماذج ذات الارتفاع الأكبر كانت أقل حساسية لتأثير الغمر، في حين أظهرت النماذج ذات الأطوال الأكبر للحافة انخفاضاً أكبر في الكفاءة. وبصورة عامة، تحافظ الهدارات المتشابكة ذات الزوايا المستديرة على أداءٍ جيد ضمن نطاق واسع من الظروف التشغيلية. وتقدم هذه النتائج فهماً جديداً لتأثير شكل الحافة ودرجة الغمر على الخصائص الهيدروليكية للهدارات المتشابكة

الكلمات المفتاحية:

الهدار المتشابك المستطيل، الأداء الهيدروليكي، معامل التصريف، مستوى الغمر

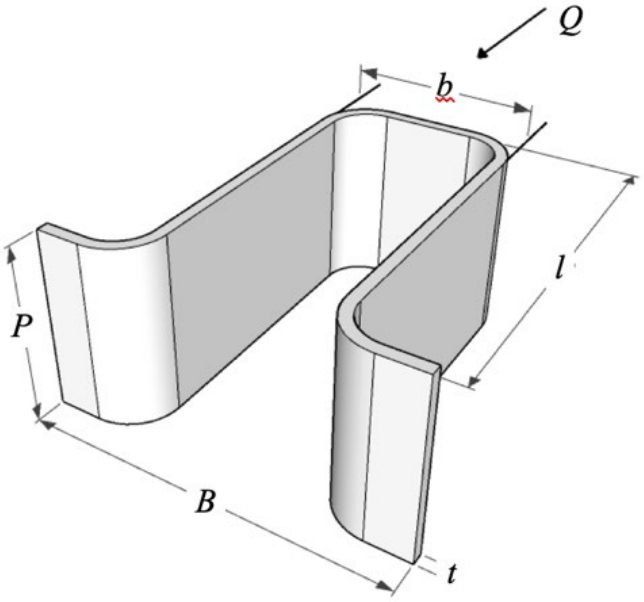

Figure 1. Isometric view of rounded-corner rectangular labyrinth weir

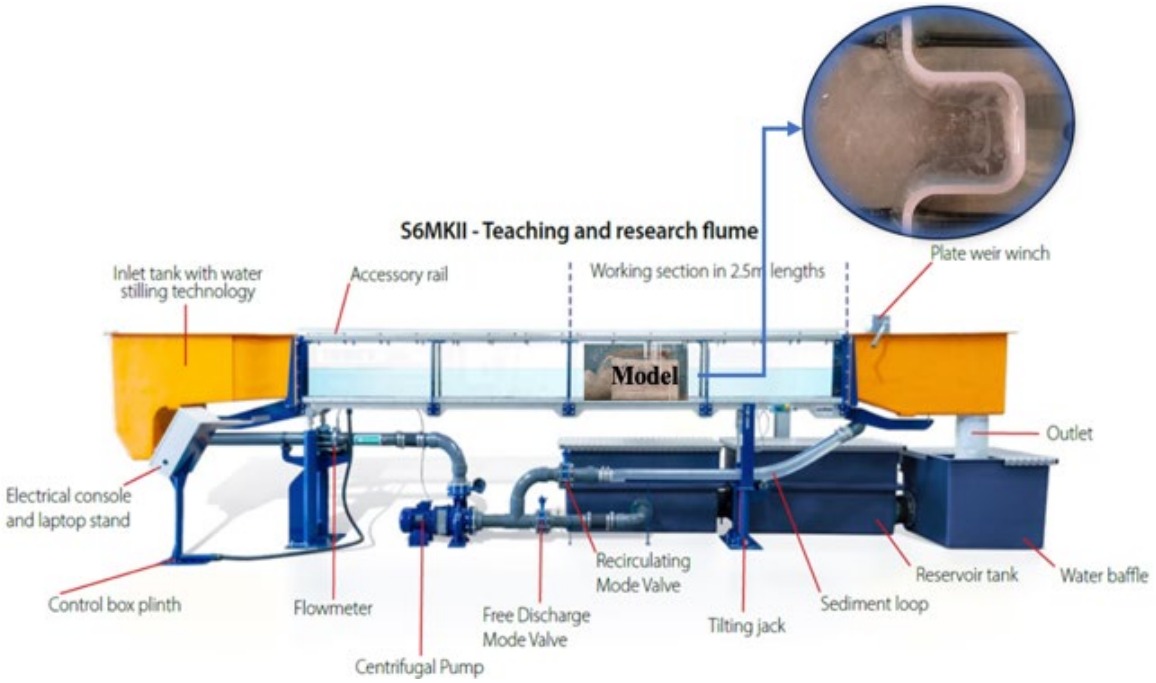

Figure 2. Armfield S6-MKII laboratory flow channel.

Table 1. Characteristics of the weir models.

Model	b (mm)	l (mm)	t (mm)	P (mm)	L_C (mm)	L_C/B	B/P
M1	160	160	10	150	533.6	2.79	2.0
M2	160	160	10	200	533.6	2.79	1.5
M3	160	160	10	250	533.6	2.79	1.2
M4	160	310	10	150	836	3.28	2.0
M5	160	310	10	200	836	3.28	1.5
M6	160	310	10	250	836	3.28	1.2
M7	160	460	10	150	1136	3.79	2.0
M8	160	460	10	200	1136	3.79	1.5
M9	160	460	10	250	1136	3.79	1.2

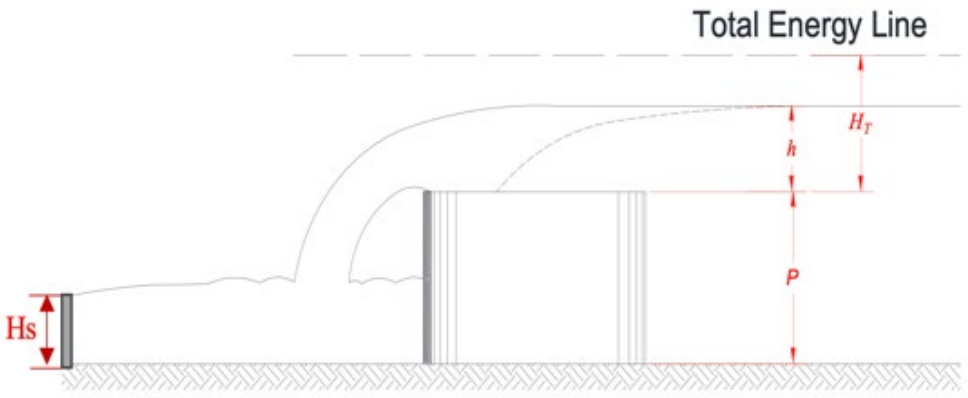

Figure 3. Schematic diagram of flow over rectangular labyrinth weir including flow parameters.

Table 2. Detail of experimental runs for free flow

Model	Free flow		
	Q, m³/s	***h, m***	$(H_T/P)^*$
M1	0.00368– 0.03252	0.002 – 0.009	0.133– 0.600
M2	0.00412– 0.03357	0.002 – 0.009	0.10–0.44
M3	0.00412– 0.02945	0.002 – 0.009	0.08– 0.32
M4	0.00295– 0.02463	0.002 – 0.009	0.133– 0.600
M5	0.00296– 0.02394	0.002 – 0.009	0.10–0.44
M6	0.00285– 0.02412	0.002 – 0.009	0.08– 0.32
M7	0.00475– 0.03231	0.002 – 0.008	0.133– 0.600
M8	0.00421– 0.03056	0.002 – 0.007	0.10–0.44
M9	0.00429– 0.03075	0.002 – 0.007	0.08– 0.32

Table 3. Detail of experimental runs for submerged flow by 50mm at D/S

Model	Submerged flow by 50mm		
	Q, m³/s	***h, m***	$(H_T/P)^*$
M1	0.00368-0.02916	0.002 – 0.009	0.133– 0.600
M2	0.00412-0.03357	0.002 – 0.009	0.10–0.44
M3	0.00412-0.02945	0.002 – 0.009	0.08– 0.32
M4	0.00295-0.02212	0.002 – 0.009	0.133– 0.600
M5	0.00296-0.02394	0.002 – 0.009	0.10–0.44
M6	0.00285-0.02412	0.002 – 0.009	0.08– 0.32
M7	0.00475-0.03231	0.002 – 0.009	0.133– 0.600
M8	0.00421-0.03056	0.002 – 0.007	0.10–0.44
M9	0.00429-0.03075	0.002 – 0.007	0.08– 0.32

Table 4. Detail of experimental runs for submerged flow by 100mm at D/S

Model	**Submerged flow by 100mm**		
	Q, m³/s	***h, m***	$(H_T/P)^*$
M1	0.00368-0.02198	0.002 – 0.009	0.133– 0.600
M2	0.00412-0.02915	0.002 – 0.009	0.10–0.44
M3	0.00412-0.02945	0.002 – 0.009	0.08– 0.32
M4	0.00295-0.01873	0.002 – 0.009	0.133– 0.600
M5	0.00296-0.02175	0.002 – 0.009	0.10–0.44
M6	0.00285-0.02412	0.002 – 0.009	0.08– 0.32
M7	0.00475-0.02338	0.002 – 0.009	0.133– 0.600
M8	0.00421-0.02957	0.002 – 0.008	0.10–0.44
M9	0.00429-0.03075	0.002 – 0.007	0.08– 0.32

Table 5. Detail of experimental runs for submerged flow by 150mm at D/S

Model	**Submerged flow by 150mm**		
	Q, m³/s	***h, m***	$(H_T/P)^*$
M1	0.00102-0.01193	0.002 – 0.009	0.133– 0.600
M2	0.00412-0.02156	0.002 – 0.009	0.10–0.44
M3	0.00412-0.02630	0.002 – 0.009	0.08– 0.32
M4	0.00084-0.01120	0.002 – 0.009	0.133– 0.600
M5	0.00296-0.01787	0.002 – 0.009	0.10–0.44
M6	0.00285-0.02206	0.002 – 0.009	0.08– 0.32
M7	0.00223-0.01277	0.003 – 0.009	0.133– 0.600
M8	0.00421-0.02066	0.002 – 0.008	0.10–0.44
M9	0.00429-0.02423	0.002 – 0.007	0.08– 0.32

* P = weir height, H_T total head over the weir, see Figure 3.

Figure 4. Photographs of the nine models, h = 70 mm.

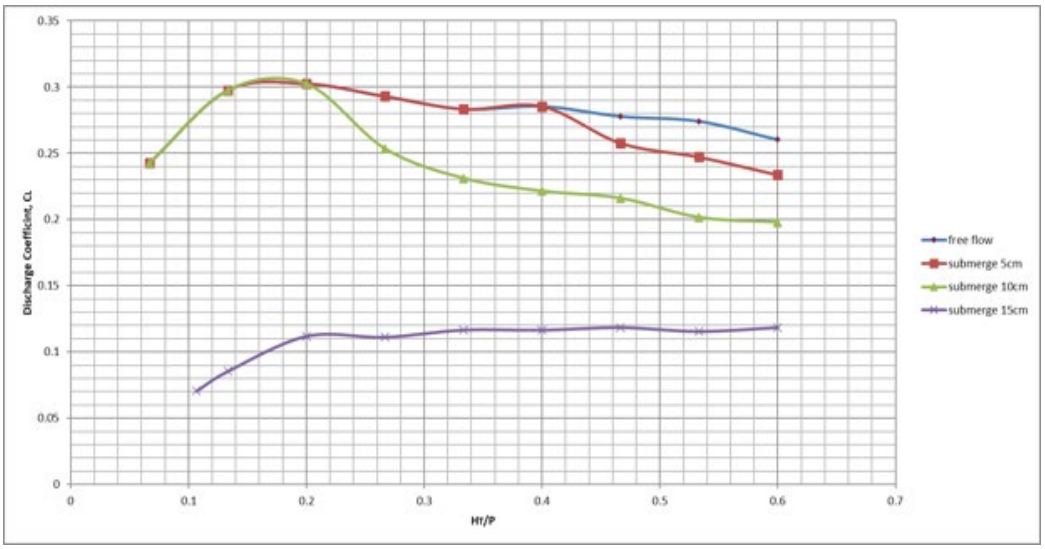

Figure 5. Discharge Coefficient, C_L, variation for M1 model (P=150 mm, l= 160 mm).

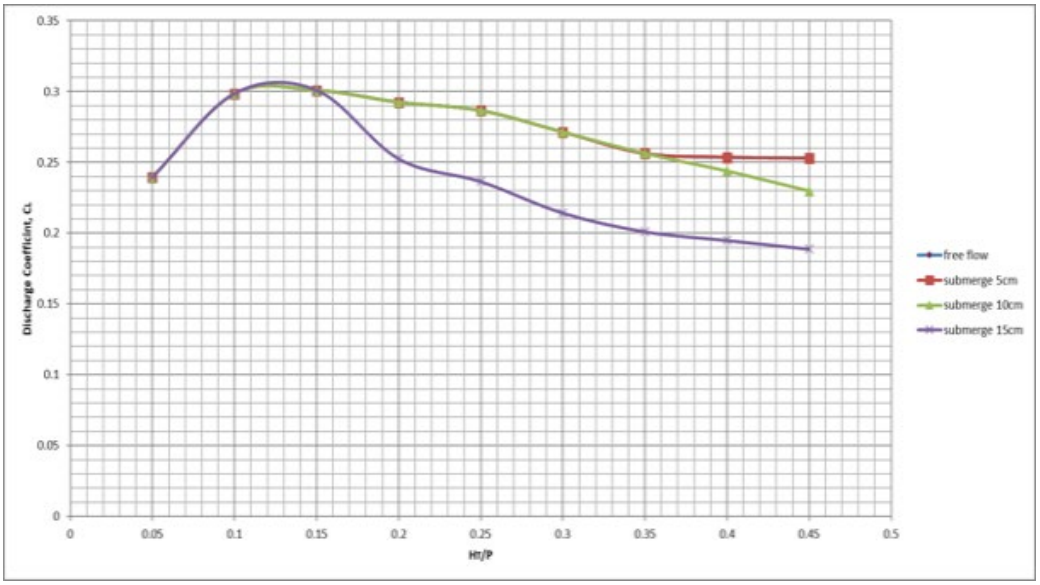

Figure 6. Discharge Coefficient, C_L, variation for M2 model (P=200 mm, l=160 mm).

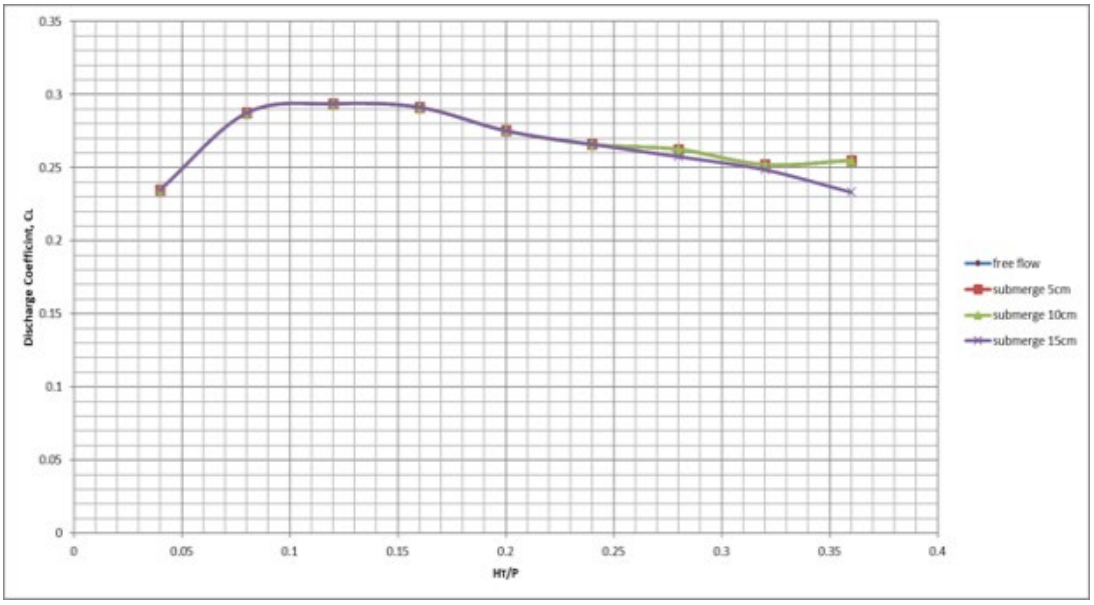

Figure 7. Discharge Coefficient, C_L, variation for M3 model (P=250 mm, l=160 mm).

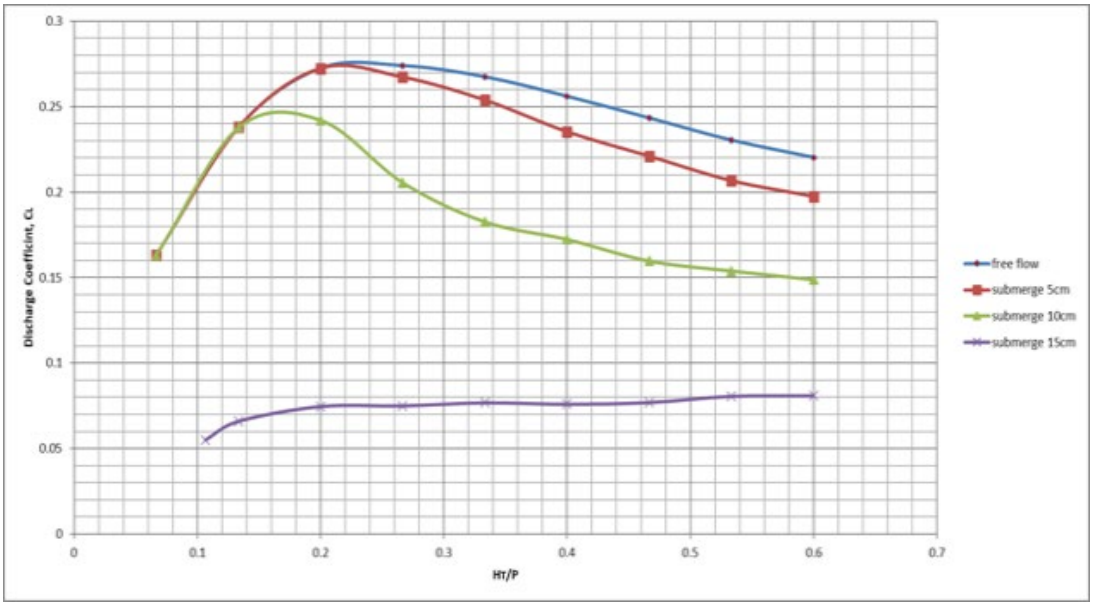

Figure *8*. Discharge Coefficient, C_L, variation for M4 model (P= 150 mm, l= 310 mm).

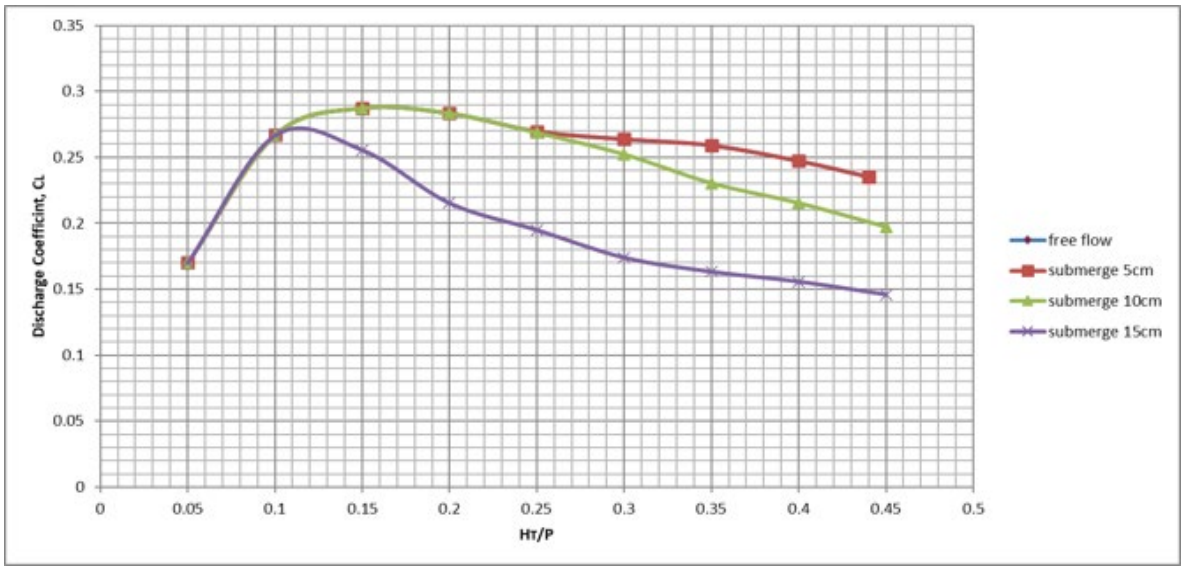

Figure *9.* Discharge Coefficient, C_L, variation for M5 model (P= 200 mm, l= 310 mm).

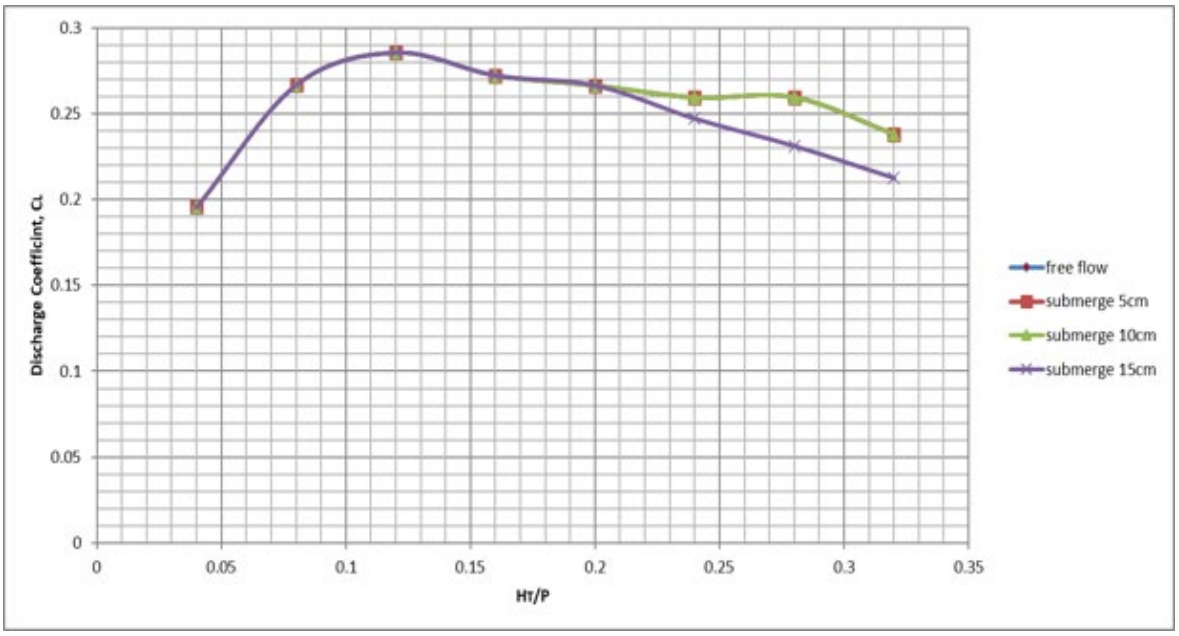

Figure *10.* Discharge Coefficient, C_L, variation for M6 model (P= 250 mm, l= 310 mm).

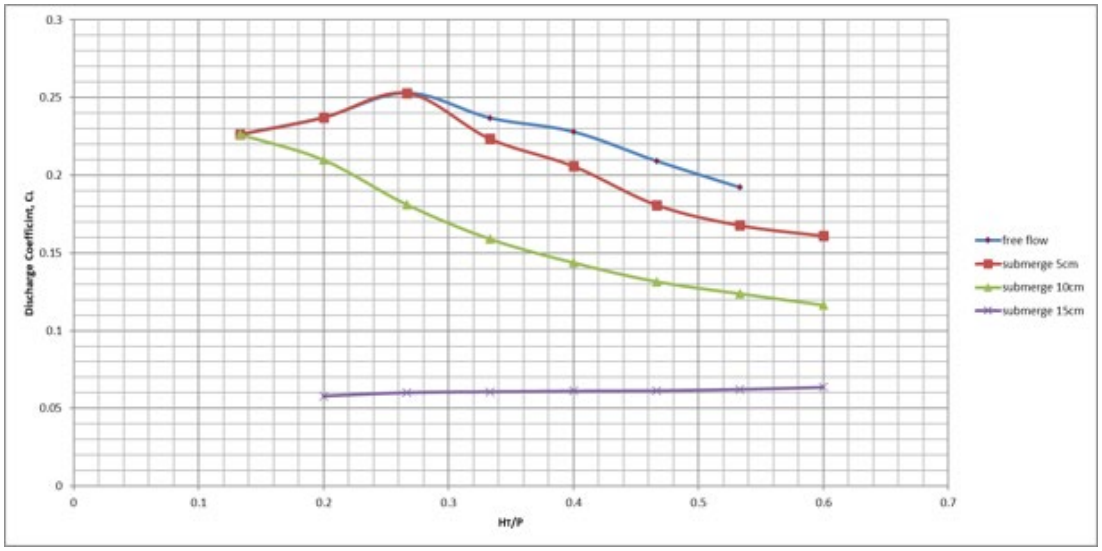

Figure 11. Discharge Coefficient, C_L, variation for M7 model (P= 150 mm, l= 460 mm).

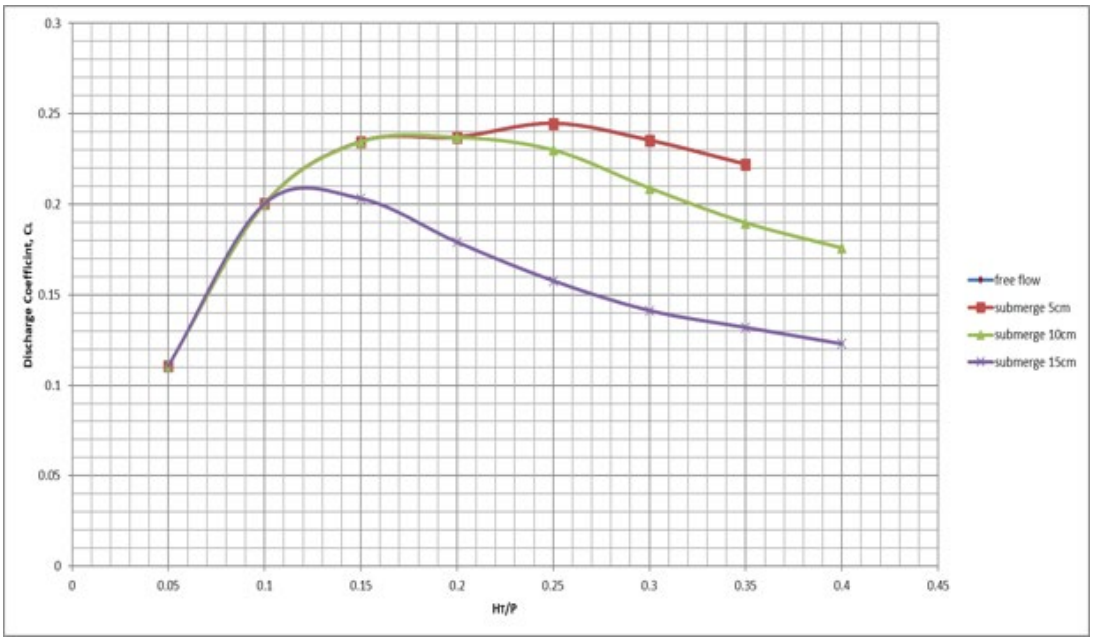

Figure 12. Discharge Coefficient, C_L, variation for M8 model (P= 200 mm, l= 460 mm)

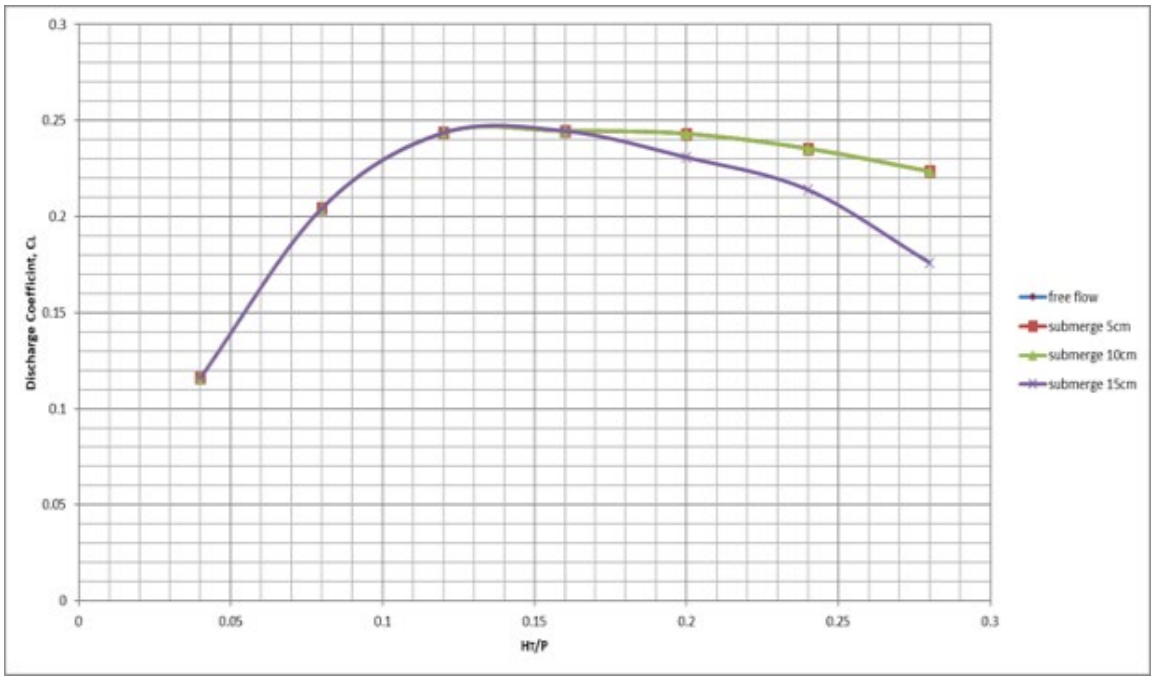

Figure 13. Discharge Coefficient, C_L, variation for M9 model (P= 250 mm, l= 460 mm).

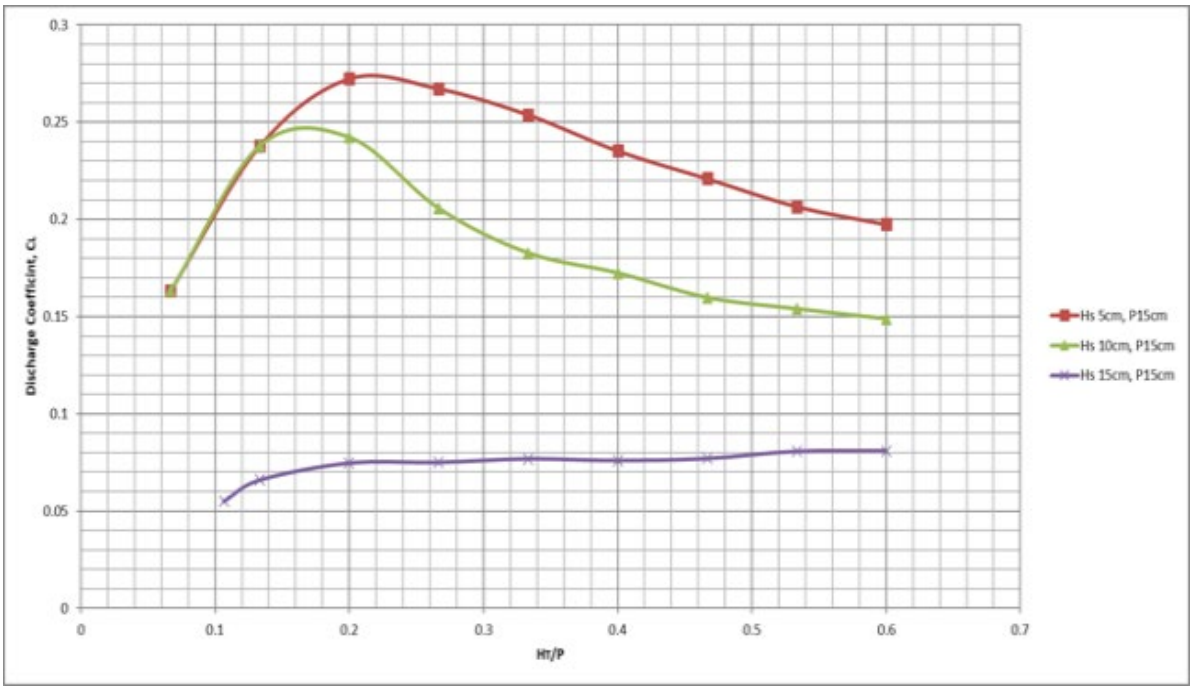

Figure 14. Discharge Coefficient, C_L, variation with H_T/P for Hs = (5, 10, 15) cm at P =15cm.